Available online at www.sciencedirect.com
ScienceDirect
Trans. Nonferrous Met. Soc. China 33(2023) 2439−2448
Transactions of Nonferrous Metals Society of China
www.tnmsc.cn

Effects of aging process on properties and precipitation kinetics of Cu−Cr−Zr alloy strips

Hai-te YANG[1*], Wen-wei-jiao WANG[1*], Chen WANG[1], Jian WANG[1], Jian-hui ZHOU[2], Chang-qing TONG[3], Jun-feng CHEN[1], Bing-shu WANG[1]

1. College of Materials Science and Engineering, Fuzhou University, Fuzhou 350108, China;
2. Fujian Zijin Copper Co., Ltd., Longyan 364200, China;
3. College of Chemistry and Materials, Longyan University, Longyan 364012, China

Received 28 December 2021; accepted 13 June 2022

Abstract: Cu−1.0Cr−0.1Zr alloy strips were prepared by solution, cold rolling and aging processes. The effects of aging process on the conductivity, mechanical properties and microstructure of the alloy were studied, and the precipitation kinetics was analyzed. The results showed that the Cu−1.0Cr−0.1Zr alloy exhibited the best comprehensive properties after aging at 430 ℃ for 180 min, with an electrical conductivity of 85.86% IACS, a hardness of HV 176.54, and a tensile strength of 552 MPa. For the samples aged at 430 ℃ from 30 to 180 min, the fcc-Cr and Cu_8Zr_3 phases grew from ~5 to ~8 nm, and the relationship between the precipitates and matrix changed from coherent to semi-coherent. In addition, the rod-like and spherical coarse particles (≥300 nm) of bcc-Cr phase were observed. The precipitation kinetics equations at different aging temperatures were established, the time−temperature−transformation (TTT) curve was plotted, and the precipitation activation energy was obtained as 65 kJ/mol.
Key words: Cu−Cr−Zr alloy; mechanical properties; conductivity; precipitates; precipitation kinetics

1 Introduction

The Cu−Cr−Zr alloy has good mechanical properties and electrical conductivity, which can be used to manufacture integrated circuit lead frame, high-speed railway contact line, electrode material and so on [1−3]. It is widely used in electronic and electrical industries, aerospace, rail transportation and other fields [4−6]. With the development of industry, the higher requirements are put forward for the comprehensive properties of Cu−Cr−Zr alloy [7].

Currently, thermomechanical treatment is the primary method for the production of Cu−Cr−Zr alloy. LIU et al [8] subjected Cu−0.55Cr−0.05Zr alloy to solid solution treatment at 1050 ℃ followed by aging at 600 ℃ for 1 h. The hardness of the obtained alloy was HV 131, and the electrical conductivity was 85.3% IACS. SOUSA et al [9] conducted equal-channel angular pressing on Cu−0.65Cr−0.08Zr alloy, which could refine the grain to 0.7 μm and produce high density dislocations in the copper matrix. After aging at 400 ℃ for 1.5 h, the conductivity and hardness of the alloy reached 92% IACS and HV 192.7. FU et al [10] studied the effects of rolling temperature, deformation degree and aging process on the properties of Cu−0.98Cr−0.057Zr alloy. It was found that a higher rolling temperature could lead to a higher conductivity and a lower tensile strength of the alloy. With increase in deformation degree, the tensile strength of the alloy increased greatly, but the conductivity did not decrease significantly.

*Hai-te YANG and Wen-wei-jian WANG contributed equally to this work
Corresponding author: Chen WANG, Fax: +86-591-22866540; Tel: +86-13809551861; E-mail: msewang@fzu.edu.cn
DOI: 10.1016/S1003-6326(23)66271-5

After rolling at room temperature with 95% deformation and aging at 450 ℃ for 1 h, the alloy obtained the best comprehensive properties of 669.1 MPa tensile strength and 74.5% IACS. MENG et al [11] adopted the process of aging Cu−0.4Cr−0.3Zr alloy at 450 ℃ for 3 h and then rolling at room temperature with 80% deformation, the tensile strength of 568 MPa and the conductivity of 75.3% IACS could be obtained. LI et al [12] used the process of aging Cu−0.67Cr−0.27Zr−0.12Ni−0.03Si−0.04Ti alloy at 450 ℃ for 2 h, and then rolling at room temperature with 80% deformation followed by aging at 400 ℃ for 1 h, the hardness and electrical conductivity of alloy were HV 197.6 and 67.4% IACS, respectively.

The strength and the conductivity of copper alloy are inconsistent with each other [13]. How to further improve the mechanical properties of copper alloys while maintaining a high level of electrical conductivity is a key problem which needs to be resolved urgently.

The Cu−Cr−Zr alloy is a precipitation strengthening alloy, so the aging process will affect the type, distribution and shape of the precipitated phases, and then affect the properties of alloy [14−16]. The evolution of precipitates containing Cr and Zr elements during aging process, as well as the precipitation kinetics, needs to be further studied. In this work, the relationships among the aging process, microstructure and properties of Cu−1.0Cr−0.1Zr alloy were analyzed through the samples aged with different process parameters. The aging precipitation kinetics equations were established, and the aging precipitation kinetics curves and the time−temperature−transformation curves were plotted. The microstructure evolution of alloy during the aging process was investigated.

2 Experimental

The Cu−1.0Cr−0.1Zr alloy used in this work is a hot-rolled plate of 1.5 mm in thickness produced by Fujian Zijin Copper Co., Ltd. The plate was solution treated at 900 ℃ for 30 min, then rapidly water quenched, followed by cold rolling at room temperature with a reduction of 85%, and then aged after cold rolling. The aging time was 1−960 min and the aging temperature was 400−520 ℃. A THV−1MD micro Vickers hardness tester was used for hardness measurement (Chinese National Standard, GB/T 4340.1—2009). The working load was 0.2 kg, the loading time was 10 s, and the average value was taken after 7 measurements. The conductivity was tested at 20 ℃ with a sigma2008 digital eddy current conductivity meter (Chinese National Standard, GB/T 32791—2016), and the average value of 7 measurements was taken. A CMT5504 universal testing machine with an extensometer was used for tensile test (Chinese National Standard, GB/T34505—2017), and the tensile rate was 0.5 mm/min. After the sample was thinned by Gatan691 ion thinning instrument, the microstructure of the sample was analyzed by a TECNAI G2F20 field emission transmission electron microscope (TEM).

3 Results and discussion

3.1 Effects of aging process on properties of alloy

Figure 1 shows the variation curves of conductivity and hardness of the Cu−1.0Cr−0.1Zr

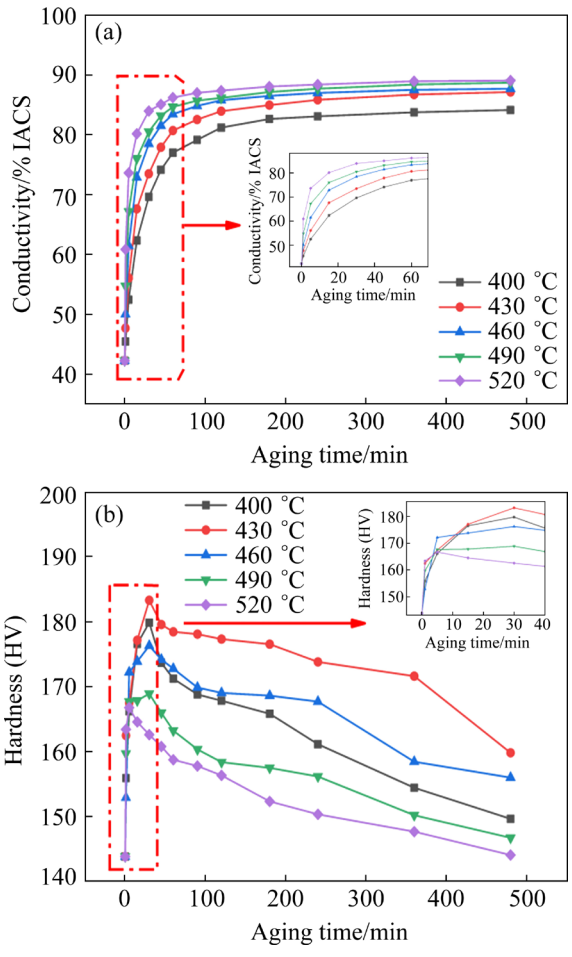

Fig. 1 Variations of electrical conductivity (a) and hardness (b) with aging time for Cu−1.0Cr−0.1Zr alloy aged at different temperatures

samples aged at different temperatures with aging time after cold rolling. As shown in Fig. 1(a), the electrical conductivity of alloy increases rapidly with the increase of time at the beginning stage of aging (1−60 min). The higher the aging temperature is, the faster the electrical conductivity increases. At the aging time of 60 min, the conductivity of alloy increases from 42.31% IACS for cold-rolled sample to 77.02%−86.24% IACS for samples aged at 400−520 ℃. With the prolongation of aging time, the increase of conductivity tends to be flat. The higher the aging temperature, the greater the maximum conductivity of the alloy. As shown in Fig. 1(b), with the increase in aging time, the hardness of Cu−1.0Cr−0.1Zr alloy increases first and then decreases. At the beginning of aging, the alloy hardness increases rapidly and reaches the peak value within 30 min. The maximum hardness is HV 179.82 for 400 ℃, HV 183.34 for 430 ℃, HV 176.38 for 460 ℃, HV 168.95 for 490 ℃ and HV 164.61 for 520 ℃, respectively. For the samples aged at 400−490 ℃, the peak aging time is 30 min, while the peak aging time of 520 ℃ is 5 min. With the increase in aging temperature, the peak hardness of alloy first increases and then decreases, reaching the maximum value of HV 183.34 after aging at 430 ℃ for 30 min.

Figure 2 shows the engineering stress−strain curves of Cu−1.0Cr−0.1Zr alloy aged at 430 ℃ for different time. As the aging time increases, the tensile strength first increases and then decreases. Compared with the cold-rolled sample, the tensile strengths of the aged samples are significantly enhanced. The sample aged for 30 min exhibits the highest tensile strength of 563 MPa, and the tensile strength of the sample aged for 180 min only decreases slightly to 552 MPa. Table 1 lists the yield strength, tensile strength and elongation of alloy aged at 430 ℃ for different time.

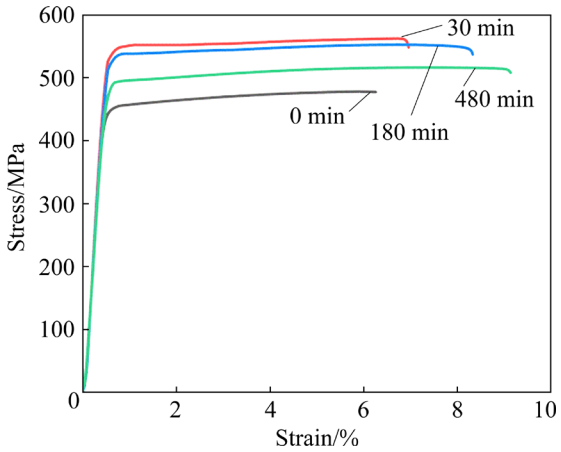

Fig. 2 Engineering stress−strain curves of Cu−1.0Cr−0.1Zr alloy aged at 430 ℃ for different time

By comprehensively comparing the conductivity, hardness and tensile strength of the samples prepared under different aging process parameters, it can be considered that the optimal aging process for Cu−1.0Cr−0.1Zr alloy is aging at 430 ℃ for 180 min. In this process, the conductivity of the alloy is 85.86% IACS, the hardness is HV 176.54, and the tensile strength is 552 MPa.

Table 1 Yield strength, tensile strength and elongation of Cu−1.0Cr−0.1Zr alloy aged at 430 ℃ for different time

Aging time/min	Yield strength/MPa	Tensile strength/MPa	Elongation/%
0	450	479	5.6
30	539	562	6.2
180	527	552	7.7
480	478	516	8.5

3.2 Effects of aging process on microstructure of alloy

Figure 3 shows the TEM bright field images of Cu−1.0Cr−0.1Zr alloy aged at 430 ℃ for 30 min. A large number of dislocation tangles and dislocation cells can be observed in Fig. 3(a). The fine precipitates with the size of 3−7 nm are dispersed in Cu matrix, as shown in Fig. 3(b). Three sets of diffraction spots corresponding to Cu matrix (M), fcc-Cr phase (P_1) and Cu_8Zr_3 phase (P_2) can be observed from the selected area electron diffraction (SAED) in Fig. 3(b). The orientation relationship among Cu matrix, fcc-Cr phase and Cu_8Zr_3 phase can be expressed as: $(1\,1\,\bar{1})_M // (1\,1\,\bar{1})_{P_1} // (\bar{1}\,1\,\bar{4})_{P_2}$ and $[1\,\bar{1}\,0]_M // [1\,\bar{1}\,0]_{P_1} // [\bar{4}0\,\bar{1}]_{P_2}$.

Figure 4(a) shows the high-resolution TEM (HRTEM) and fast Fourier transformation (FFT) images of Cu−1.0Cr−0.1Zr alloy aged at 430 ℃ for 30 min. There are two sets of diffraction spots in the FFT image, which are Cu matrix and fcc-Cr phase. Figures 4(b) and (c) are the inverse FFT (IFFT) images corresponding to the $(\bar{1}\,\bar{1}\,1)$ and (002) crystal planes of Cu matrix, respectively. Only a small amount of misfit dislocations can be observed, indicating that the relationship between the fcc-Cr phase and matrix phase is almost coherent [17,18].

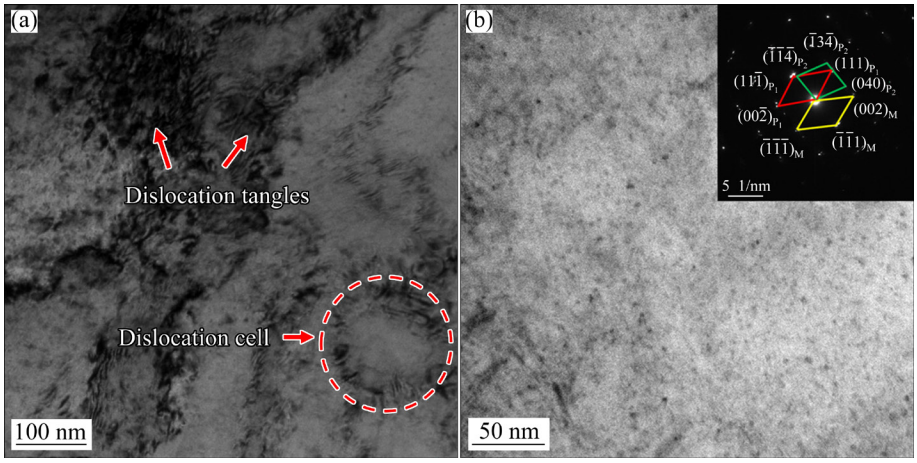

Fig. 3 TEM bright field images of Cu−1.0Cr−0.1Zr alloy aged at 430 ℃ for 30 min: (a) Dislocations; (b) Precipitates and corresponding SAED

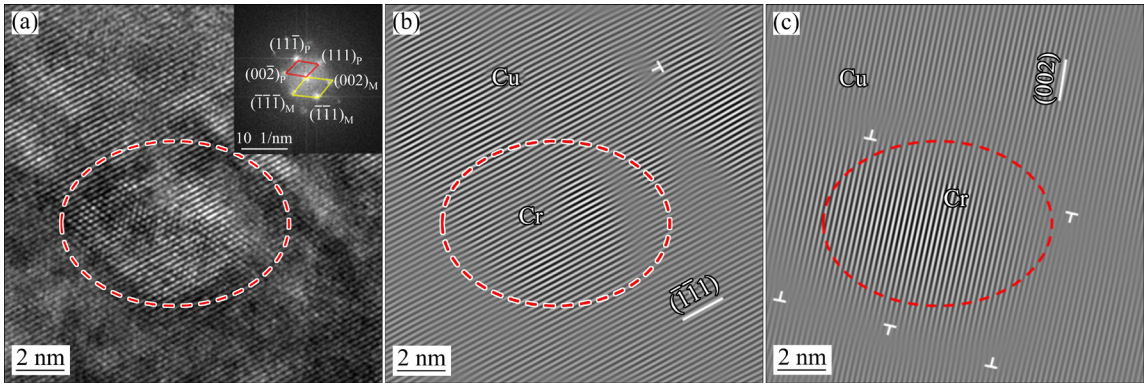

Fig. 4 HRTEM image of Cr precipitate with FFT of Cu−1.0Cr−0.1Zr alloy aged at 430 ℃ for 30 min (a), IFFT image (b) of (a) using only $(\bar{1}\,\bar{1}\,1)$ plane, and IFFT image (c) of (a) using only (002) plane

Therefore, the movement of electrons between the matrix and the precipitates is less affected, and the scattering effect of the precipitates on the electrons is not obvious.

Figures 5(a) and (b) show the TEM bright field images of Cu−1.0Cr−0.1Zr alloy aged at 430 ℃ for 180 min. The density and size of the precipitates in the Cu matrix are increased compared with the sample aged for 30 min, and the particle size is 3−12 nm. Figures 5(c) and (f) show the HRTEM and FFT images corresponding to Regions 1 and 2 in Fig. 5(b), respectively. The types of precipitates observed from the FFT are fcc-Cr phase and Cu_8Zr_3 phase. Figures 5(d) and (e) are the IFFT images of $(\bar{1}\,\bar{1}\,1)$ and (002) crystal planes of Cu matrix in Fig. 5(c), respectively. The number of misfit dislocations is greater than that in Figs. 4(b) and (c), indicating that the fcc-Cr phase is semi-coherent with the matrix. Figures 5(g) and (h) are the IFFT images of $(\bar{1}\,\bar{1}\,1)$ and (002) crystal planes of Cu matrix in Fig. 5(f), respectively. Some misfit dislocations can be observed, which also indicates that the Cu_8Zr_3 phase is semi-coherent with the matrix.

With the extension of aging time, the solid solution atoms (Cr,Zr) gradually precipitate from the copper matrix and then grow up. Therefore, the conductivity of Cu−1.0Cr−0.1Zr alloy increases with the progress of precipitation. However, with the growth of precipitates, the relationship between precipitate phase and matrix phase changes from coherent to semi-coherent, which may be one of the reasons for the slight decrease in hardness and tensile strength of the alloy [19]. Furthermore, the growth of precipitates would lead to the reduced pinning effect of precipitates on dislocations [20], which also decreases the hardness and strength of alloy.

Not only fine precipitates (3−12 nm), but also rod and spherical coarse precipitates can be

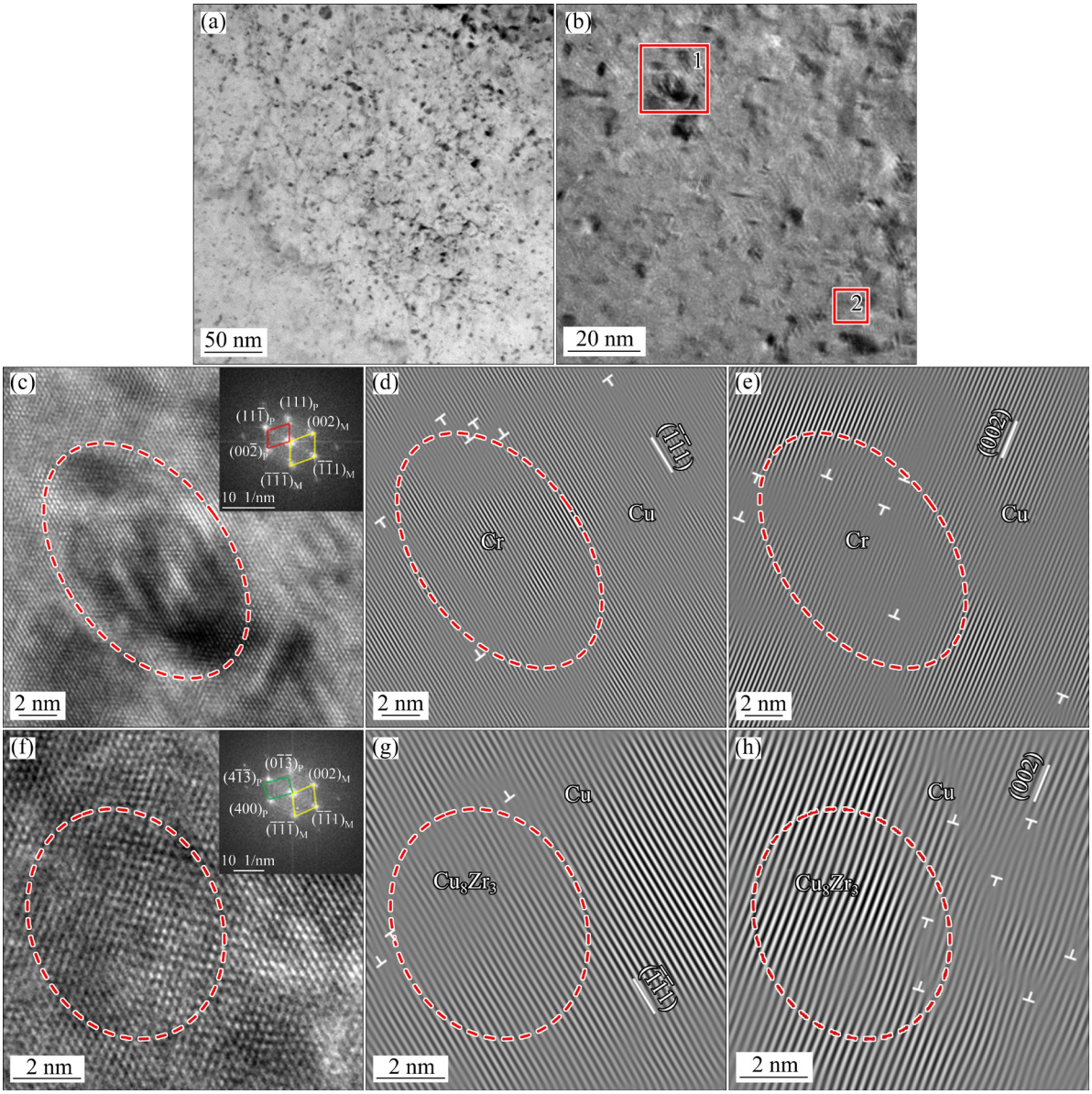

Fig. 5 (a, b) TEM bright field images of Cu−1.0Cr−0.1Zr alloy aged at 430 ℃ for 180 min; (c, f) HRTEM and FFT images corresponding to red squares 1 and 2 in (b); (d, e) IFFT images of (c) using $(\bar{1}\,\bar{1}\,1)$ and (002) planes, respectively; (g, h) IFFT images of (f) using $(\bar{1}\,\bar{1}\,1)$ and (002) planes, respectively

observed in Cu−1.0Cr−0.1Zr alloy aged at 430 ℃ for 180 min. Figures 6(a) and (c) show the TEM images of rod and spherical particles, respectively. The rod-like precipitation particles are about 900 nm in length and 200 nm in width, and the spherical precipitation particles are about 300 nm in diameter. Figures 6(b) and (d) correspond to the selected area electron diffraction of rod-like particles and spherical particles, respectively. Although the two particles have different shapes, they are the same bcc-Cr phase. This implies that there may be a transition from the fcc structure to the bcc structure during the growth of Cr precipitates. As shown in Fig. 6(c), the obvious contrast difference can be observed in the coarse spherical bcc-Cr phase. Figure 6(e) shows the HRTEM image corresponding to Fig. 6(c). Figure 6(f) is the FFT image corresponding to the red square in Fig. 6(e). Two sets of diffraction spots corresponding to bcc-Cr phase and Cu_8Zr_3 phase can be observed from Fig. 6(f). This means that the spherical bcc-Cr phase and the Cu_8Zr_3 phase coexist. In addition, the existence of coarse precipitates is also one of the reasons for the slight decrease in hardness and tensile strength of the alloy.

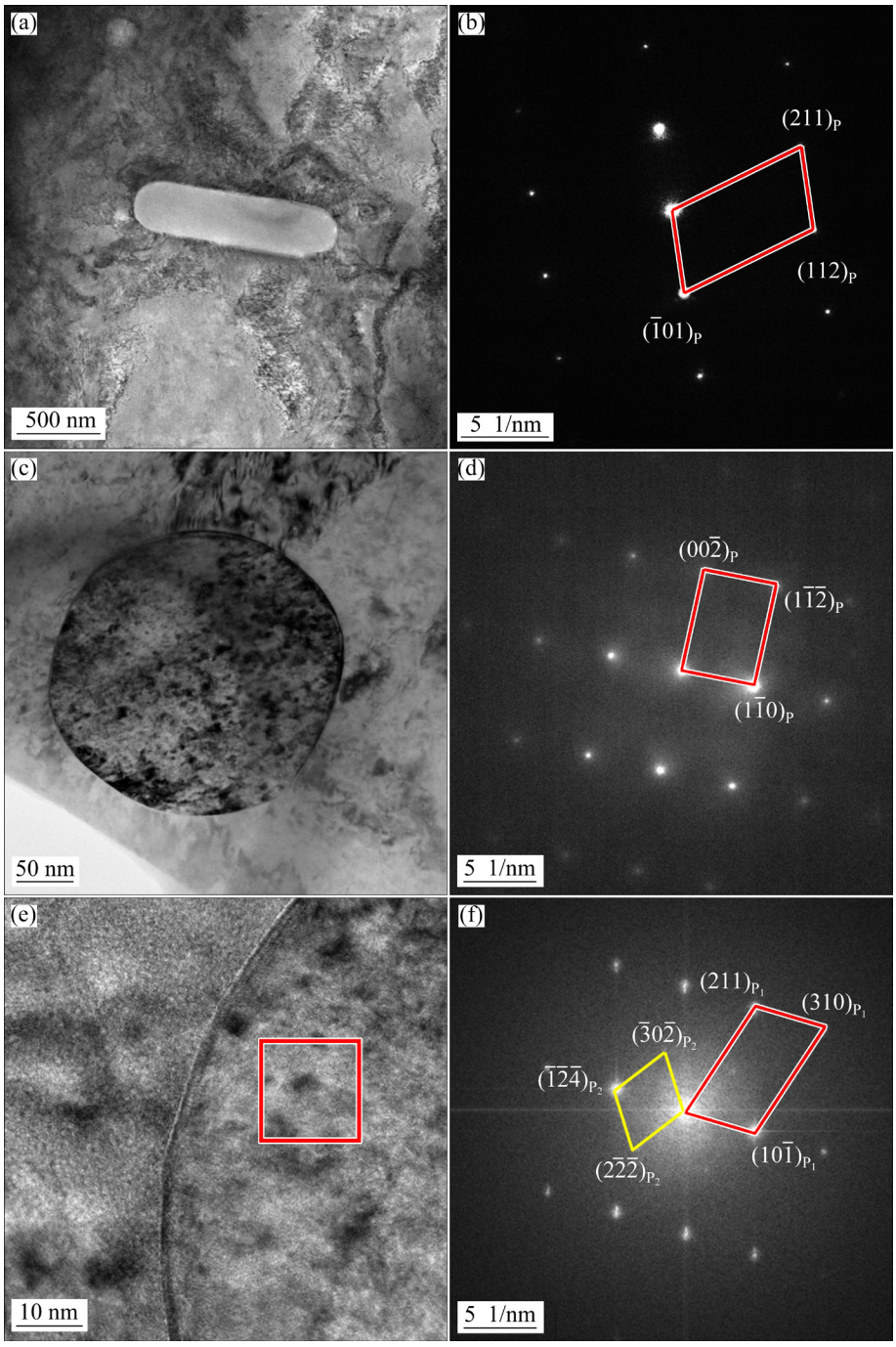

Fig. 6 TEM bright field images of Cu−1.0Cr−0.1Zr alloy aged at 430 ℃ for 180 min (a, c), SAED image (b) for (a), SAED image (d) for (c), HRTEM image (e) for (c), and FFT image (f) corresponding to red square in (e)

3.3 Precipitation kinetics analysis of alloy

During the aging process of Cu−1.0Cr−0.1Zr alloy, Cr and Zr elements precipitate from the copper matrix in the form of precipitated phases, which can lead to the change in electrical conductivity. The volume fraction of precipitates, f, is defined as [21]

$$f = \frac{V_t}{V_e} \tag{1}$$

where V_e is the equilibrium volume of precipitates formed per unit volume of the matrix at the end of precipitation aging at a certain temperature, and V_t is the volume of precipitates formed per unit volume of the matrix at a certain time aging at the same temperature with V_e. Before aging process, V_t=0, f=0. After long-term aging, the conductivity of the alloy almost does not change, so at this moment V_t=V_e, f=1.

The Matthiesen's rule [22,23] shows that the electrical conductivity (τ) is linearly correlated with the volume fraction of precipitates (f), and the expression is

$$\tau = \tau_0 + Af \tag{2}$$

where τ_0 is the conductivity of the alloy before aging, at this time f=0, τ=τ_0. At the end of precipitation, f=1, the conductivity reaches the maximum value, τ_{max}=τ_0+A. In this work, the conductivity of alloy hardly increases after aging for 960 min, which is considered to be the end of precipitation. The volume fraction of precipitates and aging time of Cu−1.0Cr−0.1Zr alloy follow the kinetics Avrami equation [24]:

$$f(t) = 1 - \exp(-Kt^n) \tag{3}$$

where K is the reaction rate constant, which is related to the nucleation and growth rate of precipitates; n is the Avrami index, which reflects the diffusion rate of atoms, and is related to phase transformation type and nucleation position of precipitates [25,26]. Based on Eq. (3), the expression of the volume fraction of precipitates with respect to aging time can be obtained:

$$\lg[\ln(1/(1-f))] = \lg K + n\lg t \tag{4}$$

The relationship diagram of lg[ln(1/(1−f))] and lg t can be obtained from Eq. (4), as shown in Fig. 7.

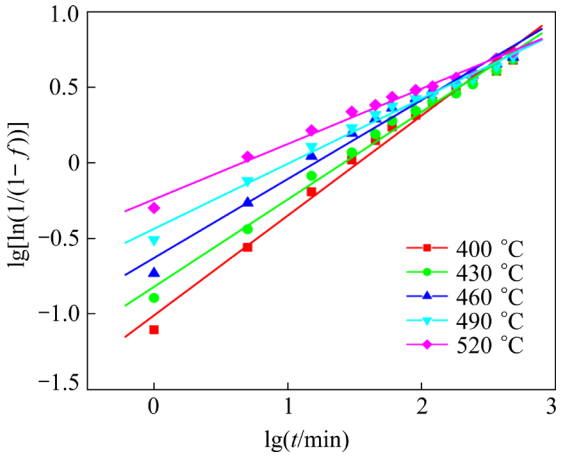

Fig. 7 Relationship between lg[ln(1/(1−f))] and lg t of Cu−1.0Cr−0.1Zr alloy aged at different temperatures

The slope n and intercept lg K can be obtained by linear fitting of the data points in Fig. 7. The n and K values corresponding to different aging temperatures are shown in Table 2. As the aging temperature increases, the K value increases significantly, indicating the increase in the precipitation rate, which is consistent with the experimental results. The value of n fluctuates between 0.50±0.17, indicating that the aging precipitation of alloy is controlled by the diffusion reaction mechanism [20]. The n value gradually decreases with the increase in aging temperature, which could be due to the increase in the diffusion rate of solute atoms.

Table 2 n and K values of Cu−1.0Cr−0.1Zr alloy aged at different temperatures

Temperature/°C	n	K
400	0.6609	0.09814
430	0.5786	0.1516
460	0.5225	0.2353
490	0.4309	0.3663
520	0.3662	0.5742

There is a competition between the nucleation and growth of the precipitates during the aging process [20]. The increase in aging temperature will enhance the thermal diffusion of solute atoms, which can promote the precipitation of solute atoms from the supersaturated Cu matrix, thus improving the nucleation rate of precipitates. The increase in the number of precipitates contributes to the increase in the alloy hardness. However, the continuous increase in aging temperature will further enhance the diffusion ability of solute atoms, which will lead to the rapid growth of precipitates, and even lead to the coarsening of precipitates. The over-sized precipitates will weaken the precipitation strengthening effect [27]. Therefore, the alloy hardness increases first and then decreases with increasing the aging temperature.

Substituting the data of Table 2 into Eq. (3), the precipitation kinetics equations of the alloys aged at 400−520 °C can be obtained:

$$f_{400°C} = 1 - \exp(-0.09814t^{0.6609}) \tag{5}$$

$$f_{430°C} = 1 - \exp(-0.1516t^{0.5786}) \tag{6}$$

$$f_{460°C} = 1 - \exp(-0.2353t^{0.5225}) \tag{7}$$

$$f_{490°C} = 1 - \exp(-0.3663t^{0.4309}) \tag{8}$$

$$f_{520°C} = 1 - \exp(-0.5742t^{0.3662}) \tag{9}$$

Figure 8 shows the precipitation kinetics curves obtained from Eqs. (5)−(9). At different aging temperatures, the precipitation rate exhibits an S-shaped trend. At the initial stage of aging, the precipitation rate is relatively slow. With the progress of aging, the precipitation rate increases rapidly. At the later stage of aging, the precipitation rate decreases gradually. It is worth noting that when the aging time is the same, the volume fraction of precipitates increases as the aging temperature increases.

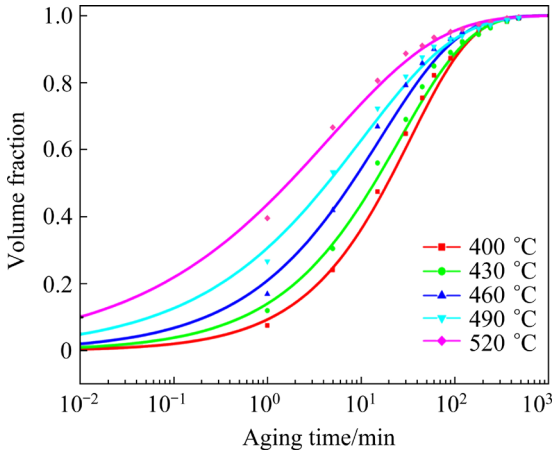

Fig. 8 Precipitation kinetics curves of Cu−1.0Cr−0.1Zr alloy aged at different temperatures

The expression of aging time (t) on the volume fraction of precipitates (f) can be obtained from Eq. (4) as

$$t=\exp\left\{\frac{1}{n}\ln\left[-\frac{\ln(1-f)}{K}\right]\right\} \tag{10}$$

In Eq. (10), the aging time corresponding to f=0.1 and f=0.9 is defined as the start time (t_s) and end time (t_e) of precipitation, respectively [26]. Based on the n and K values in Table 2, the t_s and t_e of samples aged at different temperatures can be calculated and plotted as the time−temperature−transformation (TTT) curve, as shown in Fig. 9.

According to Fig. 9, with the increase in aging temperature, the start and end time of precipitation process is advanced, and the total time required for precipitation process is reduced. The activation energy can be calculated according to the Arrhenius equation as [25,28]

$$K=K_0\exp\left(-\frac{E_a}{RT}\right) \tag{11}$$

where E_a is the activation energy of precipitation; K_0 is the frequency factor; T is the aging temperature; R is the gas molar constant, 8.314 J/(mol·K). According to Eq. (11), the following Eq. (12) can be obtained:

$$\ln K=\ln K_0-\frac{E_a}{RT} \tag{12}$$

Based on the K values and their corresponding temperatures in Table 2, the relationship between ln K and $1/T$ can be obtained, as shown in Fig. 10. According to the slope of the straight line in Fig. 10, it can be calculated that the activation energy of precipitation for Cu−1.0Cr−0.1Zr alloy is 65 kJ/mol.

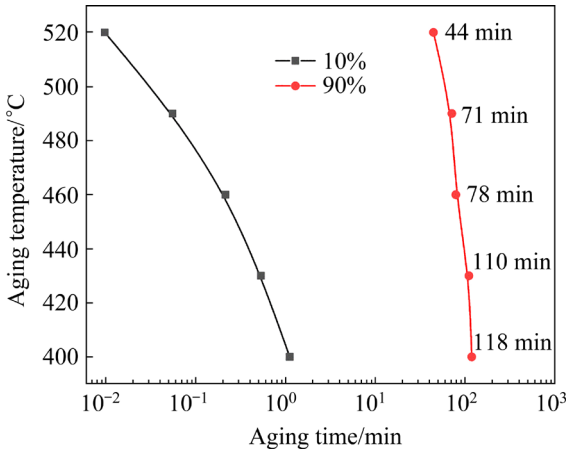

Fig. 9 TTT curve of Cu−1.0Cr−0.1Zr alloy

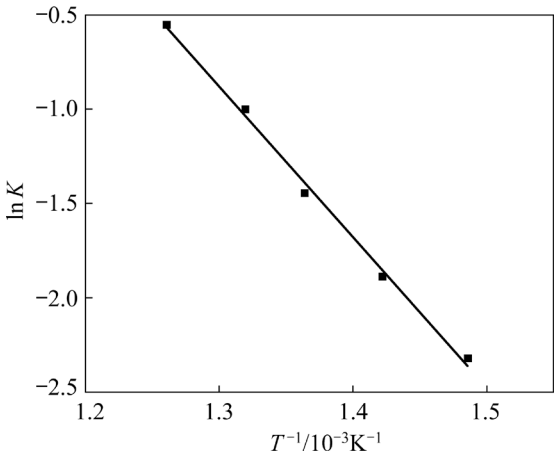

Fig. 10 Plot of ln K against $1/T$

4 Conclusions

(1) The electrical conductivity of Cu−1.0Cr−0.1Zr alloy increases with the increase of aging time at different temperatures. The higher the aging temperature is, the faster the conductivity increases. The hardness first increases and then decreases with

the increase in aging time. The optimum aging process is aging at 430 ℃ for 180 min, with an electrical conductivity of 85.86% IACS, a hardness of HV 176.54, and a tensile strength of 552 MPa.

(2) After aging at 430 ℃ for 30 min, two finely dispersed precipitation phases (~5 nm) of fcc-Cr and Cu_8Zr_3 are observed in the sample. The fcc-Cr phase is coherent with the Cu matrix. After aging at 430 ℃ for 180 min, the fcc-Cr and Cu_8Zr_3 phases grow up (~8 nm), the relationship between the fcc-Cr phase and Cu matrix changes from coherent to semi-coherent, and the Cu_8Zr_3 phase presents a semi-coherent relationship with the Cu matrix. At the same time, the coarse bcc-Cr phase (≥300 nm) can be observed in the alloy, which presents the rod-like and spherical shapes.

(3) According to the changes in electrical conductivity under different aging parameters, the precipitation kinetics equations at different aging temperatures are established, the time−temperature−transformation curve is drawn, and the precipitation activation energy of the alloy is 65 kJ/mol.

Acknowledgments

This work was financially supported by the Regional Development Project of Fujian Province, China (No. 2021H4026), the Key Project of Science and Technology Innovation of Fujian Province, China (No. 2021-113), the Joint Research Fund for Industry and University of Fujian Province, China (No. 2017H6016), and the Qimai Science and Technology Innovation Project of Shanghang County, China (No. 2017SQM044).

References

[1] SINGH R, SINGH S, KANIGALPULA P K C, SAINI J S. Electron beam welding of precipitation hardened CuCrZr alloy: Modeling and experimentation [J]. Transactions of Nonferrous Metals Society of China, 2020, 30: 2156−2169.

[2] WANG Zhi-qiang, ZHONG Yun-bo, RAO Xian-jun, WANG Chao, WANG Jiang, ZHANG Zeng-guang, REN Wei-li, REN Zhong-ming. Electrical and mechanical properties of Cu−Cr−Zr alloy aged under imposed direct continuous current [J]. Transactions of Nonferrous Metals Society of China, 2012, 22: 1106−1111.

[3] FENG Hui, JIANG Hai-chang, YAN De-sheng, RONG Li-jian. Effect of continuous extrusion on the microstructure and mechanical properties of a CuCrZr alloy [J]. Materials Science and Engineering: A, 2013, 582: 219−224.

[4] DALAN F C, de LIMA ANDREANI G F, TRAVESSA D N, FAIZOV I A, FAIZOVA S, CARDOSO K R. Effect of ECAP processing on distribution of second phase particles, hardness and electrical conductivity of Cu−0.81Cr−0.07Zr alloy [J]. Transactions of Nonferrous Metals Society of China, 2022, 32: 217−232.

[5] ZHANG Bei, ZHANG Zhi-guo, LI Wei. Mechanical properties, electrical conductivity and microstructure of CuCrZr alloys treated with thermal stretch process [J]. Transactions of Nonferrous Metals Society of China, 2015, 25: 2285−2292.

[6] ZHANG Shao-jian, LI Ren-geng, KANG Hui-jun, CHEN Zong-ning, WANG Wei, ZOU Cun-lei, LI Ting-ju, WANG Tong-min. A high strength and high electrical conductivity Cu−Cr−Zr alloy fabricated by cryorolling and intermediate aging treatment [J]. Materials Science and Engineering: A, 2017, 680: 108−114.

[7] DU Yi-bo, ZHOU Yan-jun, SONG Ke-xing, HUANG Tao, HUI D, LIU Hai-tao, CHENG Chu, YANG Jing-zhao, NIU Li-ye, GUO Hui-wen. Zr-containing precipitate evolution and its effect on the mechanical properties of Cu−Cr−Zr alloys [J]. Journal of Materials Research and Technology, 2021, 14: 1451−1458.

[8] LIU Jia-bin, HOU Meng-lian, YANG Hui-ya, XIE Hong-bin, YANG Chao, ZHANG Jin-dong, FENG Qiong, WANG Li-tian, MENG Liang, WANG Hong-tao. In-situ TEM study of the dynamic interactions between dislocations and precipitates in a Cu−Cr−Zr alloy [J]. Journal of Alloys and Compounds, 2018, 765: 560−568.

[9] SOUSA T G, de BRITO MOURA I A, COSTA GARCIA FILHO F, MONTEIRO S N, BRANDÃO L P. Combining severe plastic deformation and precipitation to enhance mechanical strength and electrical conductivity of Cu−0.65Cr−0.08Zr alloy [J]. Journal of Materials Research and Technology, 2020, 9(3): 5953−5961.

[10] FU Hua-dong, XU Sheng, LI Wei, XIE Jian-xin, ZHAO Hong-bin, PAN Zhi-jun. Effect of rolling and aging processes on microstructure and properties of Cu−Cr−Zr alloy [J]. Materials Science and Engineering: A, 2017, 700: 107−115.

[11] MENG Ao, NIE Jin-feng, WEI Kang, KANG Hui-jun, LIU Zhuang-jia, ZHAO Yong-hao. Optimization of strength, ductility and electrical conductivity of a Cu−Cr−Zr alloy by cold rolling and aging treatment [J]. Vacuum, 2019, 167: 329−335.

[12] LI Jia-zhi, DING Hua, LI Bao-mian. Study on the variation of properties of Cu−Cr−Zr alloy by different rolling and aging sequence [J]. Materials Science and Engineering A, 2021, 802: 140413.

[13] YANG Hui-ya, MA Zi-chao, LEI Chen-hui, MENG Liang, FANG You-tong, LIU Jia-bin, WANG Hong-tao. High strength and high conductivity Cu alloys: A review [J]. Science China Technological Sciences, 2020, 63(12): 2505−2517.

[14] SUN Xing-long, JIE Jin-chuan, WANG Tong-min, LI Ting-ju. Effect of two-step cryorolling and aging on mechanical and electrical properties of a Cu−Cr−Ni−Si alloy for lead frames applications [J]. Materials Science and Engineering: A, 2021, 809: 140521.

[15] WATANABE C, MONZEN R, TAZAKI K. Mechanical properties of Cu−Cr system alloys with and without Zr and

Ag [J]. Journal of Materials Science, 2008, 43(3): 813−819.
[16] MISHNEV R, SHAKHOVA I, BELYAKOV A, KAIBYSHEV R. Deformation microstructures, strengthening mechanisms, and electrical conductivity in a Cu−Cr−Zr alloy [J]. Materials Science and Engineering: A, 2015, 629: 29−40.
[17] LI Ming-yang, HU Pei, ZHANG Yi-min, CHANG Yong-qin. Enhancing performance of the CuCrZrTiV alloys through increasing recrystallization resistance and two-step thermomechanical treatments [J]. Journal of Nuclear Materials, 2021, 543: 152482.
[18] SHEN De-peng, XU Na, GONG Meng-ying, LI Ping, ZHOU Hong-bo, TONG Weiping, WILDE G. Improved tensile strength and electrical conductivity in Cu−Cr−Zr alloys by controlling the precipitation behavior through severe warm rolling [J]. Journal of Materials Science, 2020, 55(26): 12499−12512.
[19] HAO Zi-fan, XIE Guo-liang, LIU Xin-hua, TAN Qing, WANG Rui. The precipitation behaviours and strengthening mechanism of a Cu−0.4wt.%Sc alloy [J]. Journal of Materials Science & Technology, 2022, 98: 1−13.
[20] HU Geng-xiang, CAI Xun, RONG Yong-hua. Foundation of material science [M]. Shanghai: Shanghai Jiao Tong University Press, 2010. (in Chinese)
[21] SU Juan-hua, LIU Ping, LI He-jun, REN Feng-zhang, DONG Qi-ming. Phase transformation in Cu−Cr−Zr−Mg alloy [J]. Materials Letters, 2007, 61(27): 4963−4966.
[22] ZHANG Yi, VOLINSKY A A, TRAN H T, CHAI Zhe, LIU Ping, TIAN Bao-hong, LIU Yong. Aging behavior and precipitates analysis of the Cu−Cr−Zr−Ce alloy [J]. Materials Science and Engineering: A, 2016, 650: 248−253.
[23] XIA Cheng-dong, JIA Yan-lin, ZHANG Wan, ZHANG Ke, DONG Qi-yi, XU Gen-ying, WANG Ming-pu. Study of deformation and aging behaviors of a hot rolled−quenched Cu−Cr−Zr−Mg−Si alloy during thermomechanical treatments [J]. Materials & Design, 2012, 39: 404−409.
[24] LEI Qian, LI Zhou, PAN Zhi-yong, WANG Ming-pu, XIAO Zhu, CHEN Chang. Dynamics of phase transformation of Cu−Ni−Si alloy with super-high strength and high conductivity during aging [J]. Transactions of Nonferrous Metals Society of China, 2010, 20: 1006−1011.
[25] FILIPPOV V V, YAGODIN D A, RYLTSEVA A A, ESTEMIROVA S, SHUNYAEV K Y. The study of eutectoid decomposition kinetics of $Cu_{50}Zr_{50}$ alloy [J]. Journal of Thermal Analysis and Calorimetry, 2017, 127(1): 773−778.
[26] GAO Ling-qing, YANG Xiao, ZHANG Xian-feng, ZHANG Yi, SUN Hui-li, LI Nan. Aging behavior and phase transformation of the Cu−0.2wt.%Zr−0.15wt.%Y alloy [J]. Vacuum, 2019, 159: 367−373.
[27] WANG Ming-pu, JIA Yan-lin, LI Zhou, GUO Ming-xing. Advanced copper alloy with high strength and conductivity [M]. Changsha: Central South University Press, 2015. (in Chinese)
[28] LIU Wang-jiang, LI Jian, CHEN Xin, JI Ming-hua, XIAO Xian-peng, WANG Hang, YANG Bin. Effect of vanadium on the microstructure and kinetics of discontinuous precipitation in Cu−3.2Ti−0.2Fe alloy [J]. Journal of Materials Research and Technology, 2021, 14: 121−136.

时效工艺对 Cu−Cr−Zr 合金带材性能和析出动力学的影响

杨海特[1]，王文委教[1]，王 晨[1]，王 健[1]，周建辉[2]，童长青[3]，陈俊锋[1]，汪炳叔[1]

1. 福州大学 材料科学与工程学院，福州 350108；
2. 福建紫金铜业有限公司，龙岩 364200；
3. 龙岩学院 化学与材料学院，龙岩 364012

摘 要：通过固溶−冷轧−时效工艺制备 Cu−1.0Cr−0.1Zr 合金带材，研究时效工艺对合金导电率、力学性能和微观结构的影响，并进行析出动力学分析。结果表明，Cu−1.0Cr−0.1Zr 合金在 430 ℃时效 180 min 后获得最佳综合性能，导电率为 85.86% IACS，硬度为 HV 176.54，抗拉强度为 552 MPa。对于在 430 ℃时效的样品，当时效时间从 30 min 增加到 180 min 时，细小的 fcc-Cr 和 Cu_8Zr_3 析出相的尺寸从~5 nm 长大到~8 nm，且析出相与铜基体的关系由共格转变为半共格。同时，还观察到 bcc-Cr 相的棒状和球状粗大颗粒(≥300 nm)。此外，建立合金在不同时效温度下的析出动力学方程，绘制等温转变 TTT 曲线，通过计算获得合金的析出激活能为 65 kJ/mol。

关键词：Cu−Cr−Zr 合金；力学性能；导电率；析出相；析出动力学

(Edited by Xiang-qun LI)